activity (Narita et al., 2000). De Crescenzo et al. (2004) used Ca^{2+} imaging to show that ryanodine receptor-mediated Ca^{2+} release in isolated nerve terminals from magnocellular hypothalamic neurons was increased by Ca^{2+}-influx-independent depolarization. In the present study, however, ryanodine had no effect on the potassium-induced increase in spontaneous IPSCs, suggesting that Ca^{2+} was not being released via this pathway.

The high K^+-induced increase in spontaneous glycine release was inhibited by U-73122, suggesting a contribution of PLC to the signaling pathway coupling high K^+-induced increase in presynaptic Ca^{2+} release. PLC is known to increase intracellular IP_3 concentration, and the inhibitory effect of high concentration of wortmannin (Fig. 6) also supported the contribution of phosphoinositide breakdown to the high K^+-induced potentiation of spontaneous IPSCs. Interestingly, Thore et al. (2004) reported that PLC activity is triggered by membrane depolarization in insulin-secreting INS-1 cells. Depolarization was also reported to stimulate IP_3 production in some cells (Liu et al., 1996; Gromada et al., 1996), but, in these studies, precise mechanism was not investigated. Furthermore, the frequency of spontaneous miniature postsynaptic currents observed in cultured retinal ganglion cells (Han et al., 2001) and in rat barrel cortex neurons (Simkus and Stricker, 2002), and catecholamine release from adrenal chromaffin cells (Augustine and Neher, 1992) are increased as a consequence of mobilization of Ca^{2+} though the IP_3 receptors, and IP_3 receptor staining was found in nerve terminals of deep cerebellar nuclei (Sharp et al., 1993). Although the involvement of PLC is consistent with involvement of this pathway in our current study, our pharmacological results did not support any contribution of IP_3 receptors to the enhanced glycine release. This may reflect the lack of suitable membrane-permeable IP_3 receptor antagonists. XeC was initially reported to be an inhibitor of IP_3 receptors (Gafni et al., 1997) but Solovyova et al. (2002) demonstrated that XeC empties the endoplasmic reticulum Ca^{2+} stores but does not inhibit IP_3-induced Ca^{2+} release. The other reported blocker of IP_3 receptors employed, 2-APB, has also been reported to inhibit the Ca^{2+}-ATPase (Missiaen et al., 2001) and transient receptor potential (TRP) channels (Xu et al., 2005).

Since the experiments were performed in the absence of extracellular Ca^{2+}, the spontaneous IPSCs observed in the present study were presumably miniature events. On the other hand, the amplitude of spontaneous IPSCs was increased during high K^+ application even in the absence of extracellular Ca^{2+}. Because the high K^+ solution had no effect on the current evoked by exogenously applied glycine, it is not likely that the changes in spontaneous ISPC amplitude resulted from a postsynaptic effect of high K^+. In addition, the rise time of spontaneous IPSCs during high K^+ application was not significantly different from that recorded under control conditions, suggesting that the large-amplitude spontaneous IPSCs did not result from spatial summation of independent events occurring at distant postsynaptic sites. Thus, it is possible to assume that the increase in spontaneous IPSC amplitude may be due to synchronous multivesicular release of glycine from single or adjacent release sites. Llano et al. (2000) have shown that large miniature GABAergic IPSCs observed in rat cerebellar Purkinje cells are due to the synchronous release of multiple vesicles regulated by Ca^{2+} release from presynaptic Ca^{2+} stores. The multivesicular release, which is dependent on presynaptic Ca^{2+} stores, has also been proposed at excitatory synapses (Sharma and Vijayaraghavan, 2003; Gordon and Bains, 2005). In these studies, the synchronized multivesicular release is also accompanied with a marked increase in the frequency of spontaneous transmitter release. In the present study, BAPTA-AM inhibited the high K^+-induced increase in the spontaneous IPSC amplitude and frequency. Thus, it may be possible that the high K^+-induced Ca^{2+} release from presynaptic stores triggered highly synchronized exocytosis of multiple readily releasable vesicles, which might generate large-amplitude spontaneous IPSCs. However, further studies are required to explore this possibility.

It has been reported that presynaptic depolarization per se modulate transmitter release in the absence of Ca^{2+}-influx (Parnas et al., 2000). Membrane depolarization has also reported to affect the affinity of some G-protein-coupled-receptors for the agonists. For example, the membrane depolarization increases the affinity of M1 muscarinic receptor and metabotropic glutamate receptor (mGluR1a) to the agonists (Ben-Chaim et al., 2003; Ohana et al., 2006). In the rat spinal cord, on the other hand, the activation of presynaptic glycine autoreceptors causes the membrane depolarization and increases Ca^{2+}-influx, which in turn increases the glycine release (Jeong et al., 2003). If these presynaptic receptors are voltage-dependent and membrane depolarization increases their affinity, the low concentration of glycine, available at the presynaptic terminals, may suffice to increase the glycine release by releasing Ca^{2+} from intracellular stores. However, the properties of presynaptic glycine receptors are largely unknown at present. Thus, further studies are needed to clarify this possibility.

CONCLUSION

In conclusion, our present results demonstrated that the extracellular high K^+ condition is able to cause a Ca^{2+}-influx independent release of Ca^{2+} from intracellular Ca^{2+} stores resulting in a marked increase in exocytosis of glycine-containing synaptic vesicles. These results may suggest that high K^+-induced presynaptic depolarization regulates transmitter release, not only by activating Ca^{2+}-influx but also by internal Ca^{2+} release. Understanding more precise pathways by which high K^+ triggers this Ca^{2+} release is an important step for fully understanding synaptic transmission in the CNS.

Acknowledgments—We thank Dr. Andrew Moorhouse (The University of New South Wales, Sydney, Australia) for critical reading of this manuscript. This work was supported by Grant-in-Aid for Scientific Research on Priority Areas—Elucidation of neural network function in the brain—from MEXT of Japan (17023035 and 18021027 to HI) and by the Ichiro Kanehara Foundation.

Please cite this article in press as: Ishibashi H, et al., High potassium-induced facilitation of glycine release from presynaptic terminals on mechanically dissociated rat spinal dorsal horn neurons in the absence . . . , Neuroscience (2007), doi: 10.1016/j.neuroscience.2007.01.018

REFERENCES

Akaike N, Moorhouse AJ (2003) Techniques: Applications of the nerve-bouton preparation in neuropharmacology. Trends Pharmacol Sci 24:44–47.

Augustine GJ, Neher E (1992) Calcium requirements for secretion in bovine chromaffin cells. J Physiol (Lond) 450:247–271.

Bardo S, Cavazzini MG, Emptage N (2006) The role of the endoplasmic reticulum Ca^{2+} store in the plasticity of central neurons. Trends Pharmacol Sci 27:78–84.

Bardo S, Robertson B, Stephens GJ (2002) Presynaptic internal Ca^{2+} stores contribute to inhibitory neurotransmitter release onto mouse cerebellar Purkinje cells. Br J Pharmacol 137:529–537.

Ben-Chaim Y, Tour O, Dascal N, Parnas I, Parnas H (2003) The M2 muscarinic G-protein-coupled receptor is voltage-sensitive. J Biol Chem 278:22482–22491.

De Crescenzo V, ZhuGe R, Velazquez-Marrero C, Lifshitz LM, Custer E, Carmichael J, Lai FA, Tuft RA, Fogarty KE, Lemos JR, Walsh JV Jr (2004) Ca^{2+} syntillas, miniature Ca^{2+} release events in terminals of hypothalamic neurons, are increased in frequency by depolarization in the absence of Ca^{2+} influx. J Neurosci 24:1226–1235.

Gafni J, Munsch JA, Lam TH, Catlin MC, Costa LG, Molinski TF, Pessah IN (1997) Xestospongins: potent membrane permeable blockers of the inositol 1,4,5-trisphosphate receptor. Neuron 19:723–733.

Gordon GR, Bains JS (2005) Noradrenaline triggers multivesicular release at glutamatergic synapse in the hypothalamus. J Neurosci 25:11385–11395.

Gromada J, Frokjaer-Jensen J, Dissing S (1996) Glucose stimulates voltage- and calcium-dependent inositol trisphosphate production and intracellular calcium mobilization in insulin-secreting beta TC3 cells. Biochem J 314:339–345.

Haage D, Karlsson U, Johansson S (1998) Heterogeneous presynaptic Ca^{2+} channel types triggering GABA release onto medial preoptic neurons from rat. J Physiol (Lond) 507:77–91.

Han MH, Kawasaki A, Wei JY, Barnstable CJ (2001) Miniature postsynaptic currents depend on Ca^{2+} released from internal stores via PLC/IP_3 pathway. Neuroreport 12:2203–2207.

Iino M (1999) Molecular aspects of the excitation-contraction coupling in skeletal muscle. Jpn J Physiol 49:325–333.

Ishibashi H, Akaike N (1995) Somatostatin modulates high-voltage-activated Ca^{2+} channels in freshly dissociated rat hippocampal neurons. J Neurophysiol 74:1028–1036.

Jeong H-J, Jang I-S, Moorhouse AJ, Akaike N (2003) Activation of presynaptic glycine receptors facilitates glycine release from presynaptic terminals synapsing onto rat spinal sacral dorsal commissural nucleus neurons. J Physiol (Lond) 550:373–383.

Jin W, Lo T-M, Loh HH, Thayer SA (1994) U73122 inhibits phospholipase C-dependent calcium mobilization in neuronal cells. Brain Res 642:237–243.

Katz B, Miledi R (1965) The effect of calcium on acetylcholine release from motor nerve terminals. Proc R Soc Lond B Biol Sci 161:496–503.

Lee SH, Kim MH, Park KH, Earm YE, Ho WK (2002) K^+-dependent Na^+/Ca^{2+} exchange is a major Ca^{2+} clearance mechanism in axon terminals of rat neurohypophysis. J Neurosci 22:6891–6899.

Liu YJ, Grapengiesser E, Gylfe E, Hellman B (1996) Crosstalk between the cAMP and inositol trisphosphate-signalling pathways in pancreatic beta-cells. Arch Biochem Biophys 334:295–302.

Llano I, Gonzárez J, Caputo C, Lai FA, Blayney LM, Tan YP, Marty A (2000) Presynaptic calcium stores underlie large-amplitude miniature IPSCs and spontaneous calcium transients. Nat Neurosci 3:1256–1265.

McDonough SI, Lampe RA, Keith RA, Bean BP (1997) Voltage-dependent inhibition of N- and P-type calcium channels by the peptide toxin omega-grammotoxin-SIA. Mol Pharmacol 52:1095–1104.

Missiaen L, Callewaert G, De Smedt H, Parys JB (2001) 2-Aminoethoxydiphenyl borate affects the inositol 1,4,5-trisphosphate receptor, the intracellular Ca^{2+} pump and the non-specific Ca^{2+} leak from the non-mitochondrial Ca^{2+} stores in permeabilized A7r5 cells. Cell Calcium 29:111–116.

Mochida S, Yokoyama CT, Kim DK, Itoh K, Catterall WA (1998) Evidence for a voltage-dependent enhancement of neurotransmitter release mediated via the synaptic protein interaction site of N-type Ca^{2+} channels. Proc Natl Acad Sci U S A 95:14523–14528.

Momiyama A, Takahashi T (1994) Calcium channels responsible for potassium-induced transmitter release at rat cerebellar synapses. J Physiol (Lond) 476:197–202.

Nabekura J, Katsurabayashi S, Kakazu Y, Shibata S, Matsubara A, Jinno S, Mizoguchi Y, Sasaki A, Ishibashi H (2004) Developmental switch from GABA to glycine release in single central synaptic terminals. Nat Neurosci 7:17–23.

Nakamura M, Jang I-S, Ishibashi H, Watanabe S, Akaike N (2003) Possible role of kainate receptor on GABAergic presynaptic nerve terminals projecting to rat substantia nigra dopaminergic neurons. J Neurophysiol 90:1662–1670.

Narita K, Akita T, Hachisuka J, Huang S-M, Ochi K, Kuba K (2000) Functional coupling of Ca^{2+} channels to ryanodine receptors at presynaptic terminals. Amplification of exocytosis and plasticity. J Gen Physiol 115:519–532.

Ohana L, Barchad O, Parnas I, Parnas H (2006) The metabotropic glutamate G-protein-coupled receptors mGluR3 and mGluR1a are voltage-sensitive. J Biol Chem 281:24204–24215.

Parnas H, Segel L, Dudel J, Parnas I (2000) Autoreceptors, membrane potential and the regulation of transmitter release. Trends Neurosci 23:60–68.

Patterson RL, van Rossum DB, Nikolaidis N, Gill DL, Snyder SH (2005) Phospholipase C-gamma: diverse roles in receptor-mediated calcium signaling. Trends Biochem Sci 30:688–697.

Peppiatt CM, Collins TJ, Mackenzie L, Conway SJ, Holmes AB, Bootman MD, Berridge MJ, Seo JT, Roderick HL (2003) 2-Aminoethoxydiphenyl borate (2-APB) antagonises inositol 1,4,5-trisphosphate-induced calcium release, inhibits calcium pumps and has a use-dependent and slowly reversible action on store-operated calcium entry channels. Cell Calcium 34:97–108.

Raiteri L, Stigliani S, Raiteri M, Bonanno G (2002) Multiple mechanisms of transmitter release evoked by "pathologically" elevated extracellular $[K^+]$: involvement of transporter reversal and mitochondrial calcium. J Neurochem 80:706–714.

Rhee JS, Ishibashi H, Akaike N (1999) Calcium channels in the GABAergic presynaptic nerve terminals projecting to Meynert neurons of the rat. J Neurochem 72:800–807.

Rios E, Brum G (1987) Involvement of dihydropyridine receptors in excitation-contraction coupling in skeletal muscle. Nature 325:717–720.

Rosenmund C, Stevens CF (1996) Definition of the readily releasable pool of vesicles at hippocampal synapses. Neuron 16:1197–1207.

Savic N, Sciancalepore M (1998) Intracellular calcium stores modulate miniature GABA-mediated synaptic currents in neonatal rat hippocampal neurons. Eur J Neurosci 10:3379–3386.

Sharma G, Vijayaraghavan S (2003) Modulation of presynaptic store calcium induces release of glutamate and postsynaptic firing. Neuron 38:929–939.

Sharp AH, McPherson PS, Dawson TM, Aoki C, Campbell KP, Snyder SH (1993) Differential immunohistochemical localization of inositol 1,4,5-trisphosphate- and ryanodine-sensitive Ca^{2+} release channels in rat brain. J Neurosci 13:3051–3063.

Simkus CR, Stricker C (2002) The contribution of intracellular calcium stores to mEPSCs recorded in layer II neurones of rat barrel cortex. J Physiol (Lond) 545:521–535.

Solovyova N, Fernyhough P, Glazner G, Verkhratsky A (2002) Xestospongin C empties the ER calcium store but does not inhibit $InsP_3$-induced Ca^{2+} release in cultured dorsal root ganglia neurones. Cell Calcium 32:49–52.

Storchak LG, Pozdnyakova NG, Himmelreich NH (1998) Differential effect of protein kinase inhibitors on calcium-dependent and calcium-independent [^{14}C]GABA release from rat brain synaptosomes. Neuroscience 85:989–997.

Please cite this article in press as: Ishibashi H, et al., High potassium-induced facilitation of glycine release from presynaptic terminals on mechanically dissociated rat spinal dorsal horn neurons in the absence . . . , Neuroscience (2007), doi: 10.1016/j.neuroscience.2007.01.018

Suh B-C, Hille B (2002) Recovery from muscarinic modulation of M current channels requires phosphatidylinositol 4,5-bisphosphate synthesis. Neuron 35:507–520.

Sutko JL, Airey JA, Welch W, Ruest L (1997) The pharmacology of ryanodine and related compounds. Pharmacol Rev 49:53–98.

Thore S, Dyachok O, Tengholm A (2004) Oscillations of phospholipase C activity triggered by depolarization and Ca^{2+} influx in insulin-secreting cells. J Biol Chem 279:19396–19400.

Treiman M, Caspersen C, Christensen SB (1998) A tool coming of age: thapsigargin as an inhibitor of sarco-endoplasmic reticulum Ca^{2+}-ATPases. Trends Pharmacol Sci 19:131–135.

Warrier A, Borges S, Dalcino D, Walters C, Wilson M (2005) Calcium from internal stores triggers GABA release from retinal amacrine cells. J Neurophysiol 94:4196–4208.

Xu SZ, Zeng F, Boulay G, Grimm C, Harteneck C, Beech DJ (2005) Block of TRPC5 channels by 2-aminoethoxydiphenyl borate: a differential, extracellular and voltage-dependent effect. Br J Pharmacol 145:405–414.

Yang F, He X-P, Russell J, Lu B (2003) Ca^{2+} influx-independent synaptic potentiation mediated by mitochondrial Na^{+}-Ca^{2+} exchanger and protein kinase C. J Cell Biol 163:511–523.

Zhang H, Craciun LC, Mirshahi T, Rohacs T, Lopes CM, Jin T, Logothetis DE (2003) PIP_2 activates KCNQ channels, and its hydrolysis underlies receptor-mediated inhibition of M currents. Neuron 37:963–975.

Zhang C, Zhou Z (2002) Ca^{2+}-independent but voltage-dependent secretion in mammalian dorsal root ganglion neurons. Nat Neurosci 5:425–430.

(Accepted 13 January 2007)

Please cite this article in press as: Ishibashi H, et al., High potassium-induced facilitation of glycine release from presynaptic terminals on mechanically dissociated rat spinal dorsal horn neurons in the absence . . . , Neuroscience (2007), doi: 10.1016/j.neuroscience.2007.01.018

Arch Histol Cytol, 69 (5): 297-310 (2006)

Age-related NADPH-diaphorase positive bodies in the lumbosacral spinal cord of aged rats*

Huibing Tan[§1,2], Jianwen He[§1], Songyan Wang[1], Kazuho Hirata[1], Zhengwei Yang[3], Akio Kuraoka[1], and Masaru Kawabuchi[1]

[1]Department of Anatomy and Cell Biology, Graduate School of Medical Sciences, Kyushu University, Fukuoka, Japan; [2]Department of Anatomy and Neurobiology, Institute of Basic Medical Sciences, Peking Union Medical College, Chinese Academy of Medical Sciences, Beijing; and [3]Morphometric Research Laboratory, North Sichuan Medical College, Sichuan, PR China

Summary. In the course of a morphological investigation of age-related changes in the rat spinal cord, using nicotinamide adenine dinucleotide phosphate-diaphorase (NADPH-d) histochemistry, we found abundant NADPH-d positive bodies, which were characteristically expressed in the aged lumbosacral spinal cord. Together with a normally stained fiber network and a few neurons, the dense, spheroidal NADPH-d positive bodies occurred in portions of the sacral dorsal spinal cords, such as the dorsal commissural nucleus, intermediolateral nuclei, and superficial dorsal horn, and were scattered throughout the dorsal white column. These NADPH-d positive bodies were occasionally observed in a fibrous structure. Two morphologically distinctive subsets of NADPH-d positive bodies were noted in the spinal cord of rats aged 8 to 36 months: 1) highly-dense spheroidal shapes with sharp edges; 2) moderately-dense spheroidal or multiangular shapes with a central "core" and a peripheral "halo". The quantitative analysis, particularly the stereological measurement, confirmed a gradual increase in the incidence and size of NADPH-d positive bodies with increasing age. With nNOS immunohistochemistry, no corresponding structures to NADPH-d positive bodies were detected in aged rats; thus NADPH-d activity is not always specific to the NO-containing neural structures. The major distribution of the NADPH-d positive bodies in the aged lumbosacral spinal cord indicates some anomalous changes in the neurite, which might account for a disturbance in the aging pathway of the autonomic and sensory nerve in the pelvic visceral organs.

Received April 6, 2006

* This work was supported by the Japan Society for the Promotion of Science, the Young Scientist Fund of the Basic Institute of Medicine (PUMC, China), and the Ministry of Education, Culture and Science of Japan (No.12000210, 12670018). In addition, Dr. Tan and Dr. Kawabuchi greatly appreciate the sponsorship given from the Heiwa-Nakashima Foundation, Tokyo, to this work.

§ The first two authors contributed equally to this work.
Address for correspondence: Kazuho Hirata, Department of Anatomy and Cell Biology, Graduate School of Medical Sciences, Kyushu University, Fukuoka 812-8582, Japan
Tel: +81-92-642-6048, Fax: +81-92-642-6050
E-mail: hirata@anat1.med.kyushu-u.ac.jp

Introduction

The lower lumbar and sacral spinal cord is important for controlling the function of the large intestine, the pelvic muscle, and the reproductive organs (Berkley *et al.*, 1993). The sacral spinal cord is intimately associated with bowel, bladder, and sexual dysfunction (Cohen *et al.*, 1991; Willis *et al.*, 1999; Berkley, 2005). The dorsal commissural nucleus (DCN) is a cellular column, about 300 μm in diameter in the transverse plane, located on the midline of the dorsal gray matter above the dorsal commissure in the L6-S1 spinal segments of rats. In comparison with the other segments of the spinal cord, the sacral DCN is the more massive gray matter. The DCN is analogous to the region of the dorsal gray commissure

(DGC) in the S1-3 segments of the cat spinal cord. This region receives the terminals of visceral afferent fibers in the pelvic nerves and somatic afferent fibers for the pudendal nerves through the Lissauer's tract (LT) and its lateral- and medial-collateral projections (McKenna and Nadelhaft, 1986; Thor *et al.*, 1989; Liu *et al.*, 1998). The retrograde transganglionic labeling of primary afferents from the bladder (Wang *et al.*, 1998), urethra (Vizzard *et al.*, 1995), and external urethral sphincter (Nadelhaft and Vera, 1996) as well as from the penile nerve (McKenna and Nadelhaft, 1986) has confirmed that the DCN/DGC is a component of the reflex pathways that control the functions of the pelvic viscera (de Groat and Steers, 1990).

Some structures of the brainstem have a neuroanatomically reciprocal relationship with the lumbosacral spinal cord (Al-Chaer *et al.*, 1996; Wang *et al.*, 1999). The sacral DCN, which is involved in the central processing of pelvic visceral information, is also implicated in the nociceptive, analgesia, and autonomic functions (Wang *et al.*, 1999). With their excitatory connections to parapsympathetic preganglionic neurons in the segments of the lumbosacral spinal cord, the pontine micturition center projections to the inhibitory interneurons in the sacral spinal cord are thought to contribute to micturition by relaxing the external urethral sphincter (Sie *et al.*, 2001). Functional evidence also indicates that the sacral DGC receives terminations from the somatic and visceral afferents (Al-Chaer *et al.*, 1996).

The nicotinamide adenine dinucleotide phosphate-diaphorase (NADPH-d) reaction is used as a marker to characterize some neuronal properties. Neurons with NADPH-d activity have been shown to exhibit colocalization with several neuropeptides in various brain nuclei (Spike *et al.*, 1993). NADPH-d activity has also been used as a marker for nitric oxide synthase (NOS) in neurons (Young *et al.*, 1997). Nitric oxide (NO) is known as an important transmitter at the peripheral synapses of the urogenital tract, particularly in the transmission of nociceptive information in the spinal cord (Rice, 1995).

Recently, Doone *et al.* (1999) have reported that NADPH-d positive cell bodies and fiber networks are densely stained in the DCN of adult animals. A large number of NADPH-d positive neurons in the spinal cord appear to be involved in visceral regulation. The NADPH-d activity of the DCN/DGC and the intermediolateral system at the segments of the lumbosacral spinal cords may have a special role in the reflexes of the pelvic organs. Changes in the neurochemical properties of these neurons after a spinal cord injury may be mediated by pathological changes in the target organs (i.e., urinary bladder) and/or spinal cord. NADPH-d positive neurons innervate most of the pelvic organs, such as the penile tissue (Tamura *et al.*, 1995), internal anal sphincter (Lynn *et al.*, 1995), and lower urinary tract (Persson *et al.*, 1993). Pelvic visceral organ-related physical and functional changes are known to occur frequently with advancing age. To the best of our knowledge, however, studies of NADPH-d histochemistry are still lacking for the lumbar and sacral spinal cord of aged rats. The main aim of this study was to investigate age-related changes in the NADPH-d positive structures of the lumbar and sacral spinal cord of the rat that may lead to impaired neural control of the pelvic organs in old age.

Materials and Methods

Animals and tissue preparation

Experiments were performed using 2- (n = 10), 4- (n = 5), 8- (n = 5), 12- (n = 5), 18- (n = 5), 24- (n = 7) and 36- (n = 5) month-old male or female Wistar rats. The mean body weight of female or male rats at each age is shown in Table 1. The animals were anesthetized with sodium pentobarbital (50 mg/kg, i.p.). The chest cavity was opened and a cannula was inserted into the ascending aorta via the left ventricle. Perfusion was performed intracardially using 100 to 150 mℓ of 0.9% NaCl, followed by 4% paraformaldehyde in a 0.1 M phosphate-buffer (PB, pH 7.4). The volume of the perfusion was approximately 300 ml in young adult rats and 500 mℓ in old rats. The spinal cords were rapidly removed and postfixed with 4% paraformaldehyde in 0.1 M PB, left at 4°C for two hours, and then placed in 25% sucrose overnight.

Staining was performed using free floating sections. The spinal cords from the cervical to coccygeal segments

Abbreviations: DCN: dorsal commissural nucleus, DGC: dorsal gray commissure, LT: Lissauer's tract, NADPH-d: nicotinamide adenine dinucleotide phosphate-diaphorase, NOS: nitric oxide synthase, NO : nitric oxide, PB: phosphate-buffer, NBT: nitro blue tetrazolium, PBS: phosphate buffered saline, LZ: Lissauer's zone, ILN: intermediolateral nuclei, ANB: age-related NADPH-d positive bodies, NAD: neuroaxonal dystrophy, DRG: dorsal root ganglia,

were cut coronally into 40 μm sections on a cryostat. Some of the spinal cords of the aged rats were cut horizontally in order to check the orientation of the NADPH-d positive bodies. To check the shape of these structures in the aged rats, coronal sections of a 100 μm thickness were also made. Most of the spinal cord sections from the young and old rats were stained and examined by NADPH-d histochemistry, with incubation in 0.1 M Tris-HCl (pH 8.0), 0.3% Triton X-100 containing 1.0 mM reduced-NADPII (Sigma, St. Louis, MO, USA) and 0.2 mM nitro blue tetrazolium (NBT, Sigma), at 37 ℃ for 90 to 120 min. The reaction was stopped by washing the sections with the phosphate buffered saline (PBS, 0.05M).

For nNOS immunohistochemistry some sections were processed using the avidin-biotin-peroxidase method. These sections were incubated first in 0.3% H_2O_2 to neutralize the endogenous peroxidase. Then a polyclonal sheep antiserum raised against recombinant rat nNOS (a gift from Dr. Emson)(1:2000) was applied to the sections for 48 h. Subsequently, the sections were incubated with biotinylated rabbit anti-sheep IgG (Jackson ImmunoReseach Lab. Inc., West Grove, PA, USA) (1:300) and then processed with peroxidase-conjugated streptavidin (Dako Inc, Kyoto)(1:500). The immunoreaction was revealed by using 3,3' diaminobenzidine (0.03% in Tris-HCl) as a chromogen. Normal rat serum, normal sheep serum or PBS was replaced with the primary antibody for control immunohistochemistry. No specific staining was observed in controls. Sections were mounted on gelatinized slides, air-dried, dehydrated, and finally coverslipped.

Some sections were processed by double-staining with NADPH-d histochemistry and nNOS immunochemistry. After NADPH-d histochemistry, the NADPH-d positive sections were maintained in PBS for the subsequent nNOS immunohistochemistry as above.

Measurement by image analysis

The sections were photographed and examined under an optical microscope. The NADPH-d positive spheroid counts were based on an examination of five to eight sections through the rostrocaudal extent of the lumbosacral spinal cord. Digital images of the sections in the sacral spinal cords were captured using a Leica CCD camera mounted on the microscope, coupled to a capture board in a PowerMac computer. These digitized images were then analyzed using NIH-Image software (version 1.62), with which each type of histochemical-positive structure was counted in a specific region.

Stereological measurement

The numerical density and diameter of NADPH-d positive bodies in the region dorsal to the central canal of the sacral spinal cord were estimated as described in earlier studies (Zhang *et al.*, 2002), using an optical dissector (West and Gundersen, 1990). In brief, sections (25 μm thick) were evaluated by using Olympus BX50 microscope. Images were captured with a video camera (WV-CP410/6; Panasonic) and transmitted to a computer. In each section, fields of observations were systematically sampled randomly using a computer-assisted motorized stage (Sichuan University, Chengdu and Smart Image Technology, Beijing) with a sampling interval of 62.5 μm in the X and Y planes. Sampling was carried out using a rectangular frame (optical dissector; 25 μm × 20 μm) generated by a software package (Smart Image Technology) and superimposed on each image at × 2679 total magnification. For each section, the focus was first on the uppermost surface, after which the focus plane was shifted down (Z-plane) in the tissue for 3 μm for the "guard space" to start evaluation. Thereafter, 15 μm of each tissue section was systematically examined by focusing down in the section at 1 μm each step to generate 15 optical sections and counting the NADPH-d

Table 1. Body weight of rats (g).

	2 M	4 M	8 M	12 M	18 M	24 M	36 M
Female	179.8 ± 17.3	275 ± 18.6	335 ± 14.5	365 ± 5.8	395 ± 13	500 ± 25.9	
(n)	(5)	(2)	(2)	(2)	(2)	(3)	(0)
Male	283.8 ± 38.8	413 ± 32.2	473.3 ± 25.2	540 ± 10	577.3 ± 22.5	632.5 ± 53.8	636 ± 46.7
(n)	(5)	(3)	(3)	(3)	(3)	(4)	(5)

M: month old

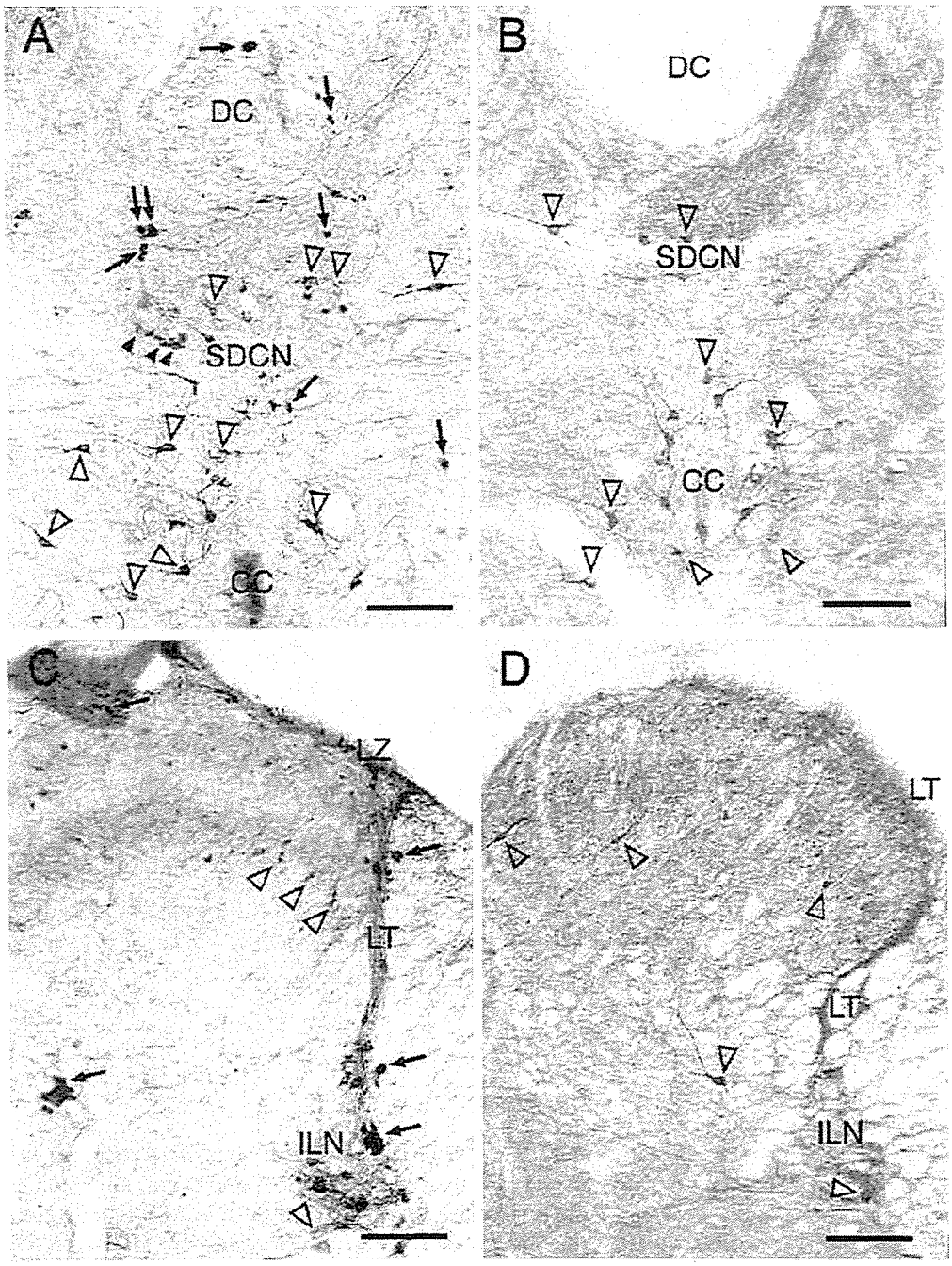

Fig. 1. Micrographs of NADPH-d reactivity in aged (24-month-old) (**A**, **C**) and young adult (2 month-old) (**B**, **D**) rats at the sacral spinal cord. **A:** The age-related NADPH-d positive bodies (ANB) in the SDCN of an aged rat. Arrows indicate highly dense spheroidal shapes with sharp edges; black arrowheads indicate moderately dense spheroidal or multiangular shapes. **B:** There are no ANB in young rats. The lateral collateral pathway of LT is visible in **C** and **D**. **C:** ANB (arrows) are accumulated in the ILN, LZ in the lateral dorsal marginal to dorsal horn, and LT of aged rats, which contrasts with the lack of ANB in young rats (**D**). Open arrowheads indicate NADPH-d positive neurons. DC: dorsal column, SDCN: sacral dorsal commissural nucleus, CC: central canal, LT: Lissauer's tract. ILN: intermediolateral nuclei. LZ: Lissauer's zone. Scale bar = 100 μm

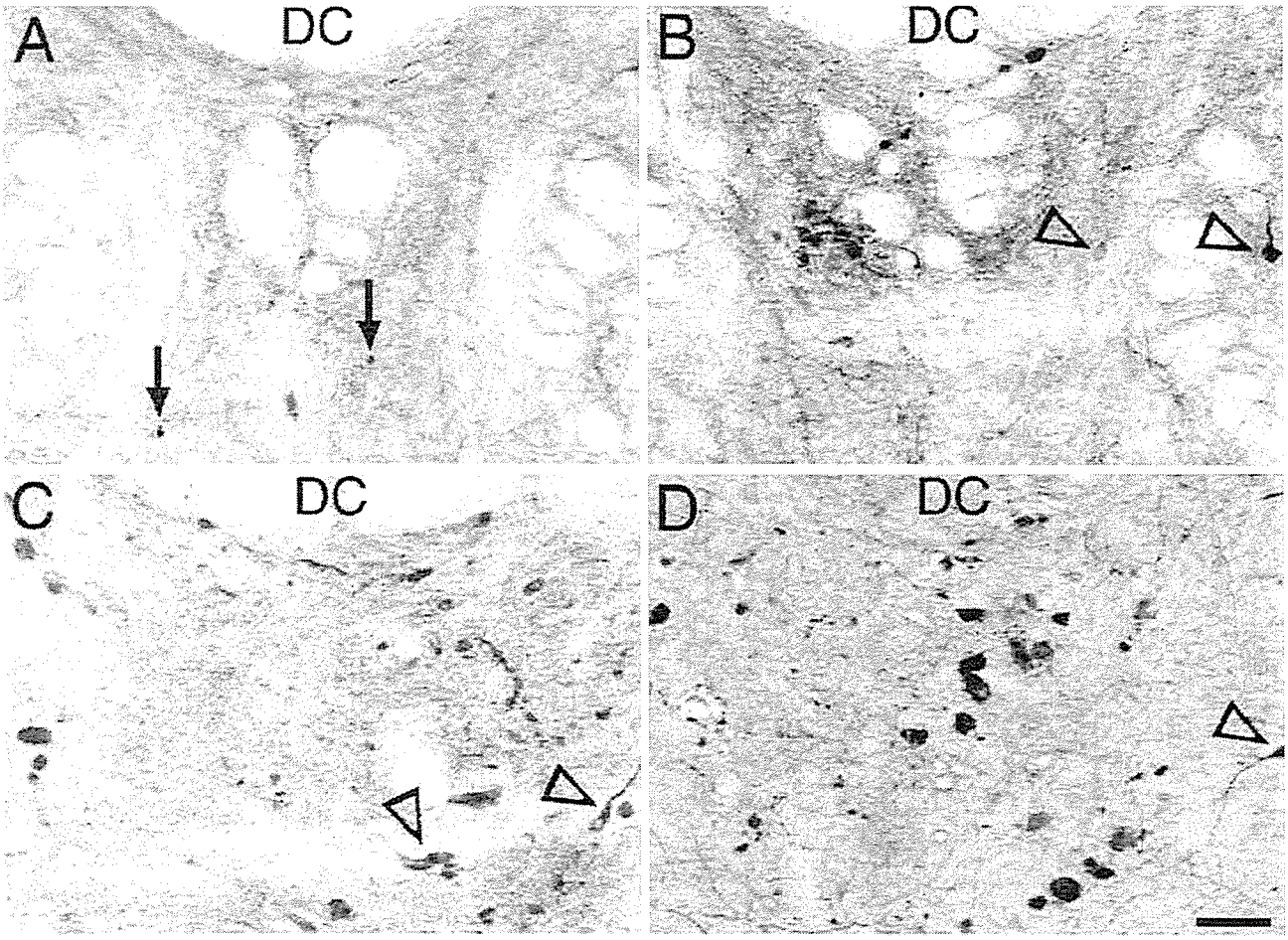

Fig. 2. The ANB between 8 and 36 months of age in sacral DCN. **A:** 8 months; **B:** 18 months; **C:** 24 months; **D:** 36 months. Arrows indicate small ANB. Open arrowheads indicate neurons. DC: dorsal column. Scale bar = 100 μm

positive bodies as they came into focus. The numerical density of these bodies was estimated by dividing their total number by the total volume of the dissectors (25 μm $\times$ 20 μm $\times$ 15 μm) used for the counting. To obtain their diameter, all round or elliptical NADPH-d positive bodies, which were to be counted according to the dissector principle were serially sectioned with a 0.5 μm distance between optical sections and the diameter of the largest profile of each NADPH-d positive body, i.e. the diameter of these bodies, was measured.

All data was entered and tabulated in Excel (Microsoft). The resulting values were presented as means $\pm$ SEM. Adobe Photoshop images were scanned directly into the program and reprinted with no noticeable degradation.

Results

All the experimental data presented here focus on the dorsal part of the lower lumber and sacral spinal cord, especially the superficial dorsal horn, Lissauer's zone (LZ), LT, the intermediolateral nuclei (ILN), in the dorsal commissure, and the region around the central canal where NADPH-d positive bodies appeared after a certain age of adult rats. The NADPH-d staining revealed a moderately dense fiber network of dendrites and axon terminals as well as moderately stained, small- and medium-sized neurons in the spinal cord of young adult rats aged 2 or 4 months (Fig. 1B, D). A positive fiber network and a few stained neurons were observed in the DCN, which is termed sacral DCN in the sacral

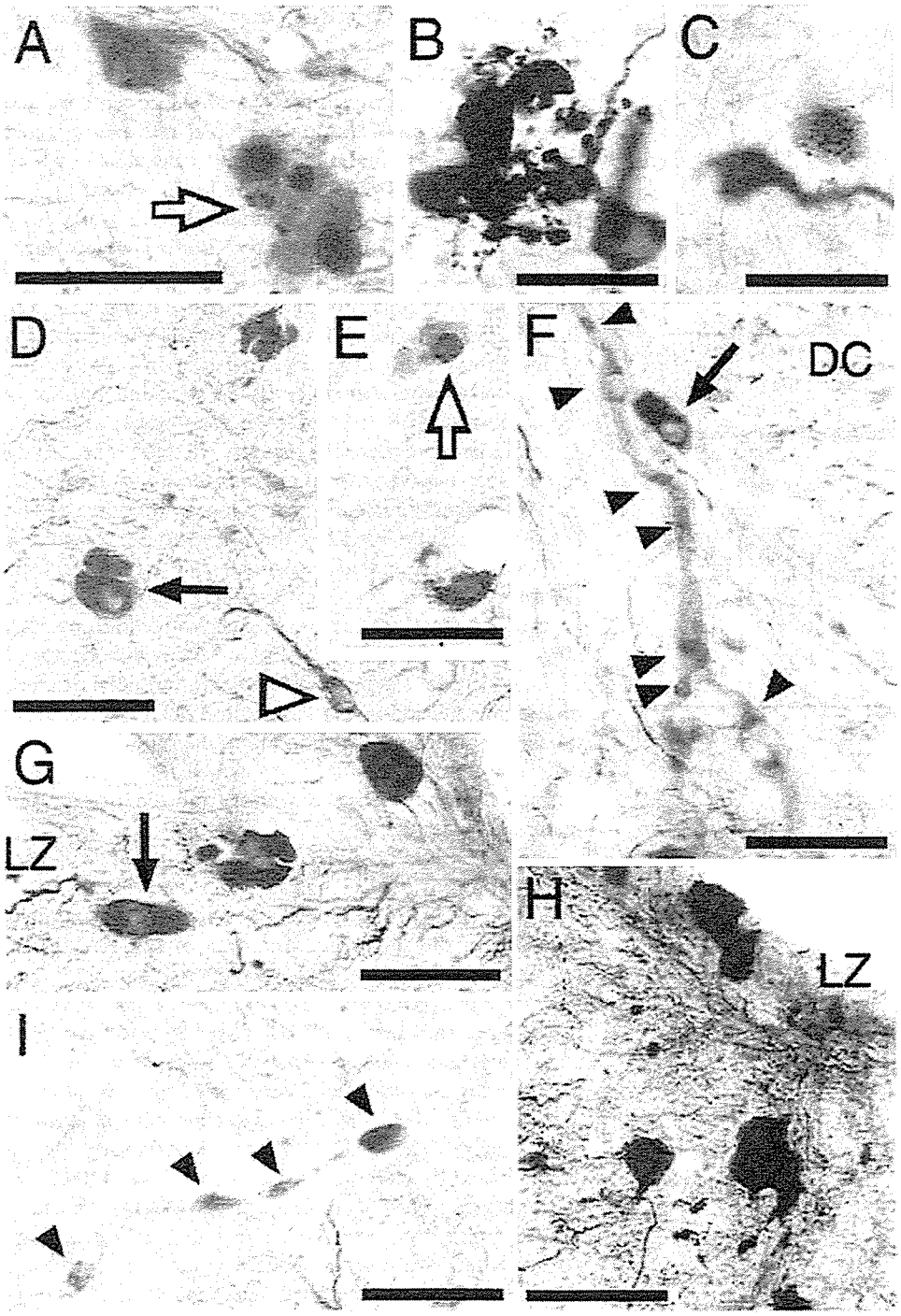

Fig. 3. Higher magnifications of ANB in sacral DCN (**A–F**, **I**) and the dorsal horn (**G**, **H**). Open arrows in **A** and **E** indicate an ANB with a central "core" and a peripheral "halo." In **B** and **C** numerous dots cluster around the ANB. In **D**, **F** and **G**, black arrows indicate ANB with vacuoles. In **F**, arrowheads indicate a moderately dense "core" in a swollen fibrous structure. In **G** and **H**, highly dense ANB in the dorsal horn show distinct outlines. In **I**, arrowheads indicate a moderately dense spheroid in a fibrous structure. DC: dorsal column, LZ: Lissauer's zone. Scale bar = 50 μm

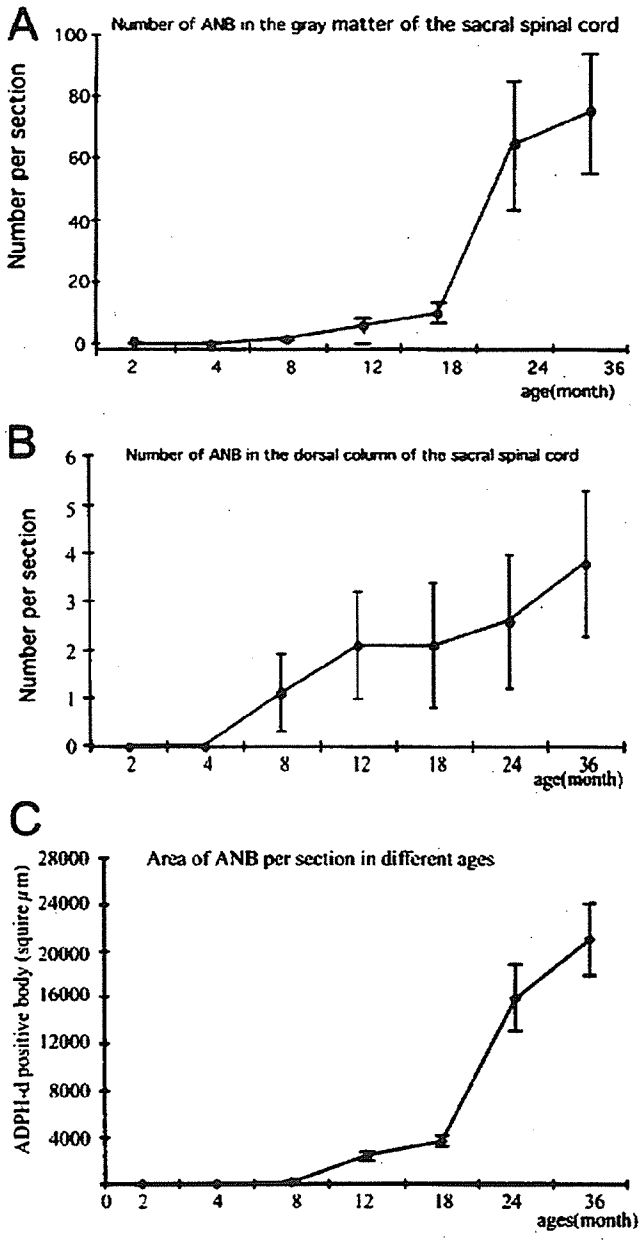

Fig. 4. Histograms showing number and area fraction (obtained by means of image analysis) of the ANB (2-dimenstional profiles) in a segment of the sacral spinal cord. **A:** Average number of ANB in the gray matter was calculated by dividing the number by the area of the gray matter in each of the sections. **B:** Average number in the DC was calculated by dividing the number by the area of the DC in each of the sections. **C:** Area fraction was the percentage of the area of the ANB in the gray matter dorsal to the CC of the sacral spinal cord.

spinal cord. These results coincide with those obtained from previous studies of the spinal cord (Doone *et al.*, 1999). In aged rats (Fig. 1A, C), the pattern of fiber-like NADPH-d activity in the superficial dorsal horn and pericentral region of the lower lumbar and sacral spinal cord was found to be quite different from that in young adult rats (Fig. 1B, D), especially in the dorsal part of the DCN (S1-S3). When compared with the young adult rats, the NADPH-d positive bodies were clearly located at the point where the primary pelvic sensory transganglionic fibers terminate (arrows in Fig. 1A, C). In addition, there were NADPH-d positive neurons with Golgi-like dendrites (open arrowheads in Fig. 1A–D). The LT was prominent in the S1-S3 segments but not in the adjacent L5-L6 and Cx1 or thoracolumbar segments. In the sacral spinal cord segments, NADPH-d reactivity in the fiber bundle extending from the LT to the sacral parasympathetic nucleus became more pronounced. The NADPH-d positive bodies in the sacral segments occurred in those fibers extending in a unique distribution from the LT through laminae I along the lateral edge of the dorsal horn to the region of the sacral parasympathetic nucleus (Fig. 1C). The NADPH-d positive bodies also occurred in the coccygeal segments of aged rats, but none of these profiles were found in the young adult rats. The NADPH-d positive bodies were also found in the root filament and occurred more frequently in the dorsal roots. There was no major difference between males and females for any features of these bodies.

The NADPH-d positive bodies, mostly highly dense, small round, or oval (Fig. 2, 6), were first observed at 8 months (Fig. 2A). Figures 2B–D show a subsequent increase in the incidence and size of the NADPH-d positive bodies in the sacral DCN after 8 months of age. The basic morphology of the NADPH-d positive bodies in the aged rats was studied. While a major group of strongly stained bodies was present in the DCN (Fig. 1A, C) in the lumbosacral spinal cord of rats aged 24 months, there were also NADPH-d positive neuronal somata with fine dendrites. The NADPH-d positive bodies often were accompanied by moderately-stained, small- and medium-sized dots (Fig.3A–C). In addition, the NADPH-d positive bodies were characterized by large- and medium-sized, spherical, or small bodies with diverse shapes. Two morphologically distinctive subsets of the NADPH-d positive bodies were noted: 1) highly-dense spheroidal or irregular shapes with sharp edges (Fig. 3B, H) (type 1); and 2) moderately-dense spheroidal or irregular shapes with a central dense "core" and peripheral "halo" (Fig. 3A, C–G, I) (type 2). The type 1, which was often intensely stained, was distributed in the dorsal part of the gray matter and dorsal column of the white matter throughout

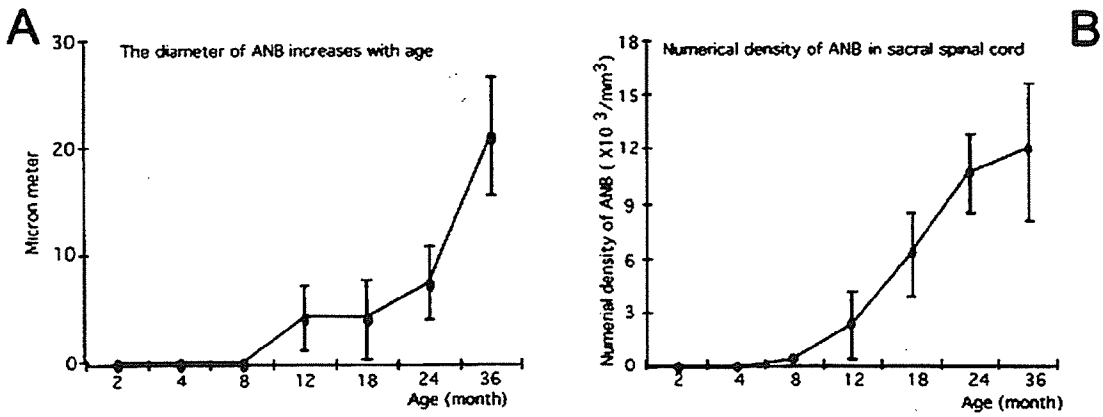

Fig. 5. Stereological quantitative analysis of the ANB in the sacral spinal cord. **A:** Diameter of ANB in the region dorsal to the CC. **B:** Numerical density of ANB in the region dorsal to the CC.

the lower lumber and sacral segments. It occasionally occurred in the lateral funiculus of the white matter as well. The type 2 was mainly localized in the gray matter of the massive dorsal part of the spinal cord. In the sacral segment, the NADPH-d positive bodies were detected in the dorsal root, dorsal horn, ILN, and the area surrounding the central canal.

Statistical data indicated that the number and area of the NADPH-d positive bodies in the transverse plane of sections progressively increased from 8 up to 18 months (Fig. 4). Thereafter their drastic increase was evident at 24 and 36 months (Fig. 4). The diameter of the transverse-sectioned NADPH-d positive bodies ranged from 2 to 36.9 μm. The time course of changes in the diameter (Fig. 5A) and numerical density (Fig. 5B) in the section of the 40–100 μm thickness were presented in the stereological data. With increasing age, the diameter increased up to a maximum of 36.9 μm (Fig. 5A).

In the horizontal (Fig. 6A, C, E–H) sections, the NADPH-d positive bodies displayed a variety of shapes. They were spheroid or fusiform in shape (Fig. 6A, C, E, F), with the longitudinally oriented fibrous form (Fig. 3F, I) (Fig. 6G, H). The longitudinally oriented swelling of the NADPH-d positive bodies occurred more frequently in the dorsal column (Fig. 6G) and dorsal horn (Fig. 6H). At higher magnifications (Fig. 6F, G, H), the size of the typical NADPH-d positive bodies was much bigger than that of the regular NADPH-d positive neuronal processes. The longest of the fibrous structures was more than 300 μm both in horizontal (Fig. 6F, G, H) and coronal sections (not shown).

In the other segments of the spinal cord of aged rats (cervical, thoracic, and rostral parts of the lumbar spinal cord), the NADPH-d positive bodies occasionally occurred in the dorsal column and dorsal horn (data not shown here). In the young rats, no NADPH-d positive bodies were found in the corresponding segments of the spinal cord. The distribution of NADPH staining and neuronal NOS-immunoreactivity in the spinal cord was investigated to evaluate the potential role of NO in lumbosacral afferent and spinal autonomic pathways as well as to compare the distribution of these two markers. No structures corresponding to NADPH-d positive bodies were detected by nNOS immunohistochemistry (Fig. 7 A–D). There were no spheroidal nNOS positive structures in the spinal cords of the aged rats. In the double-stained sections, there were three subgrouped neurons: both single labelings of the NADPH-d positive neurons (open arrowheads in Fig. 7A–D) and nNOS-immunoreactive neurons (black arrowheads in Fig. 7A–D), and double-labeling neurons (open arrows in Fig. 7 A, C, D). The NADPH-d positive bodies in aged rats were confirmed to be negative for nNOS (black arrows in Fig. 7 A–C).

Discussion

Age-related changes in NADPH-d were examined in the lumbosacral spinal cord across almost the entire rat life span. The NADPH-d positive bodies with unique morphology first appeared in the sacral DCN, LZ, dorsal horn, LT, ILN, and dorsal column in 8–12 month-old rats. Statistical data indicated that they progressively increased in number and area with age. Thus our study

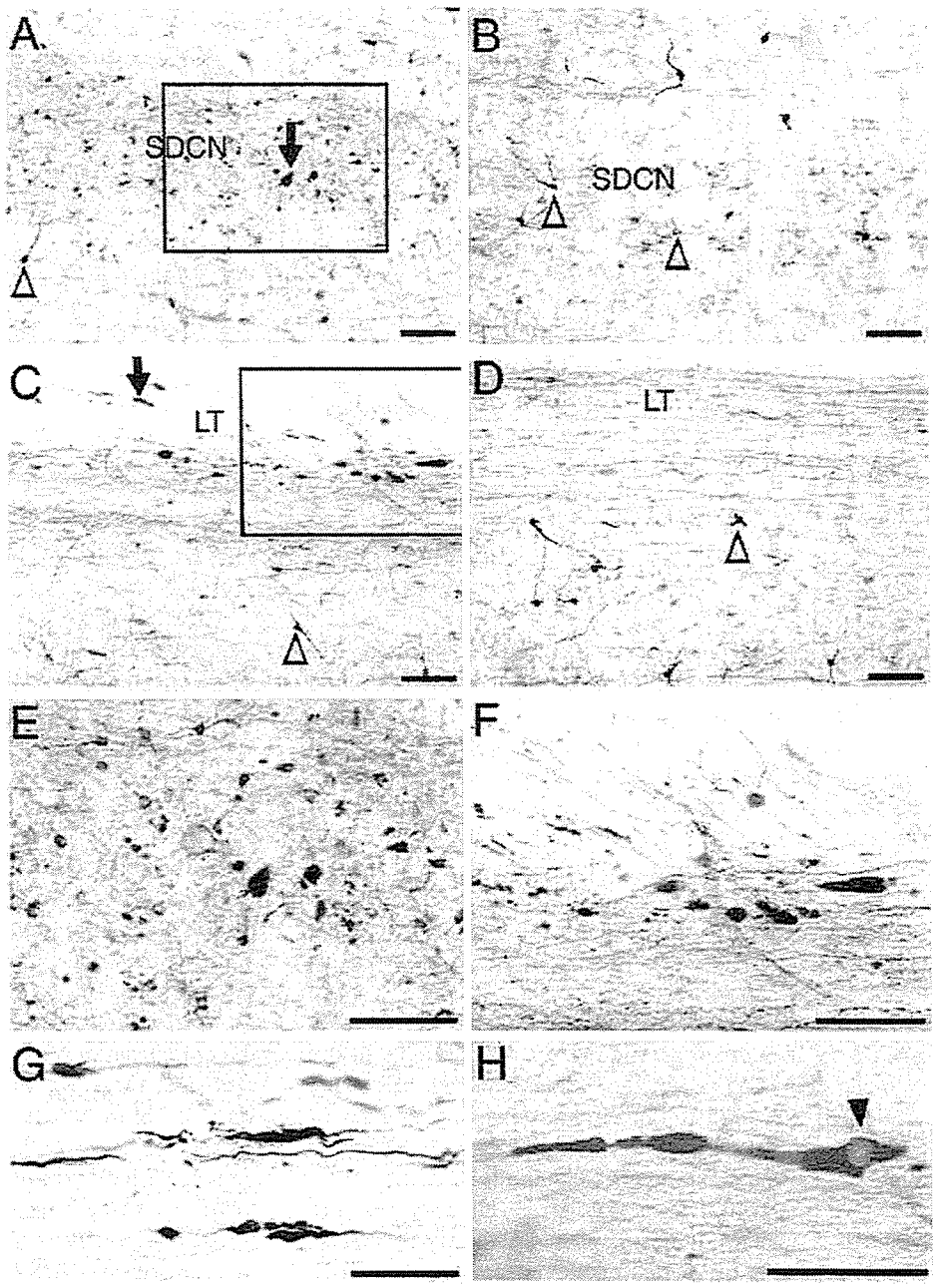

Fig. 6. Horizontal sections of 24-month-old rats (**A**, **C**, **E–H**) in comparison with those of 2-month-old rats (**B**, **D**). **A** and **C** show horizontal sections taken at the same levels as **B** and **D**, respectively. Note abundant ANB in sacral DCN (**A**) and LT (**C**). **E** shows a higher magnification from **inset A**, while **F** shows that from **inset C**. A longitudinally oriented NADPH-d positive fibrous structure is shown at the level of the DC (**G**) and dorsal horn (**H**). Black arrows: ANB, open arrowheads: NADPH-d positive neurons, black arrowhead: a vacuole in the NADPH-d positive fibrous structure. SDCN: sacral dorsal commissural nucleus, LT: Lissauer's tract. Scale bar = 100 μm

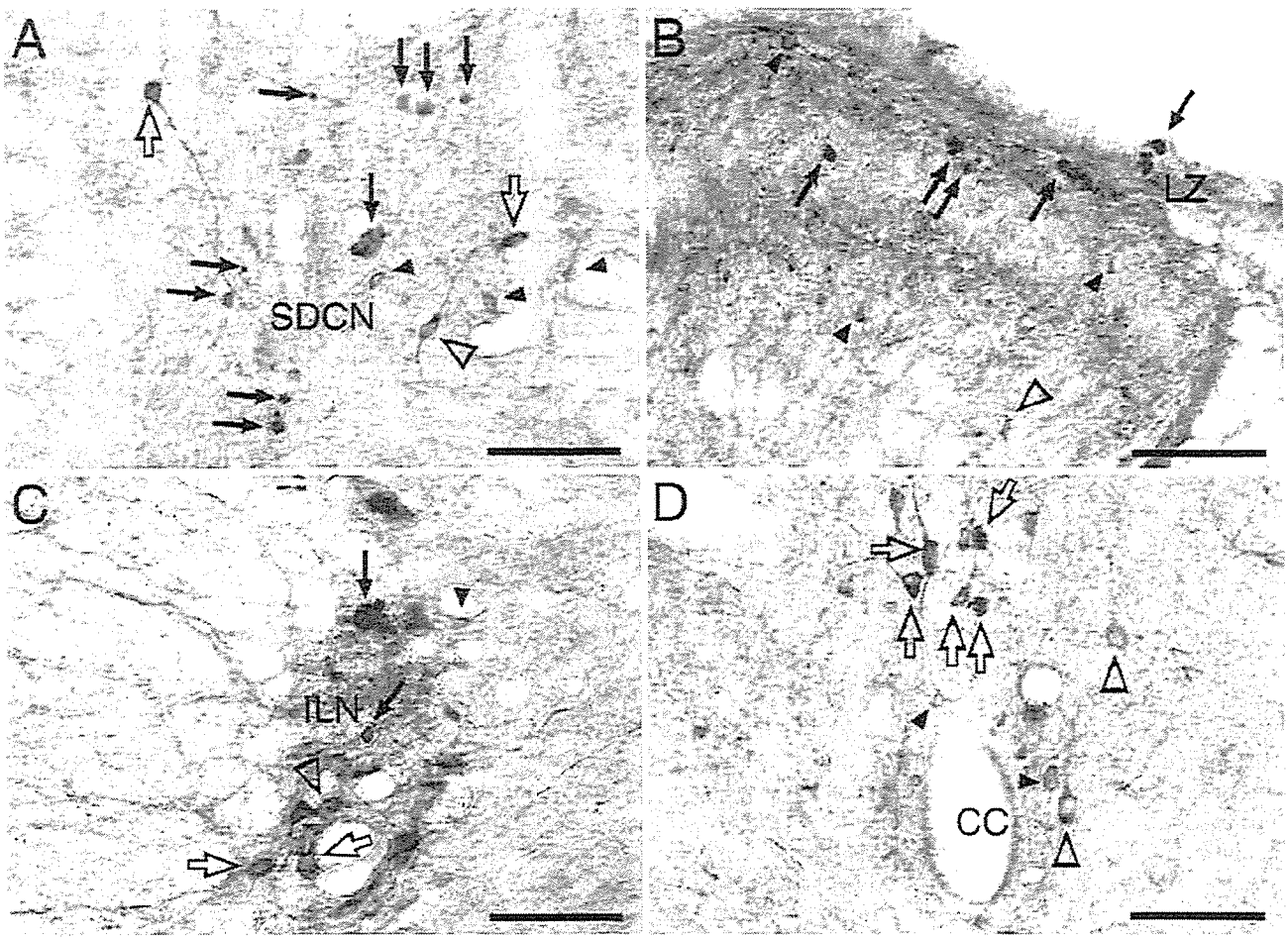

Fig. 7. Double-staining of NADPH-d histochemistry combined with nNOS immunohistochemistry in an 18-month-old rat. **A:** sacral DCN; **B:** dorsal horn; **C:** ILN; **D:** area around the CC. The ANB (black arrows) are positive for NADPH-d and negative for nNOS. Black arrowheads: single-labeled nNOS-positive neurons, open arrows: double-labeled neurons, open arrowheads: single labeled NADPH-d positive neurons. SDCN: sacral dorsal commissural nucleus, LZ: Lissauer's zone, ILN: intermediolateral nuclei, CC: central canal. Scale bar = 100 μm

revealed a specific occurrence of the age-related NADPH-d positive bodies (ANB) in dorsal part of the lumbosacral spinal cord. The sacral DCN receives terminations from the somatic and visceral afferents (Honda, 1985; Al-Chaer *et al.*, 1996) and the parasympathetic preganglionic neuronal somata are located in the ILN. The ANB were observed in both regions. Additionally, this segment of the spinal cord is known to be associated with bowel, bladder, and sexual dysfunction. Recently, Santer *et al.* (2002) demonstrated that the sympathetic preganglionic neuron populations that project into the major pelvic ganglion, and the spinal inputs that they receive, exhibit a number of degenerative changes in aged rats (24 months old) which were not seen in the parasympathetic preganglionic neuronal populations. However, the distribution of the ANB overlapped both the efferent and afferent pathways of the autonomic system, which regulates the pelvic organs.

The ANB occurred in the DCN of the lumbosacral spinal cord. These spheroids also occurred throughout the dorsal column at all levels of the spinal cord, particularly at the lumbosacral spinal cord (Fig. 1A, 6G). Recently, projections from the DCN have been implicated in visceral nociception as discrete lesions of the dorsal

column have been found to relieve pelvic pain in patients (Willis *et al.*, 1999). This clinical evidence is supported by anatomical studies using rats and monkeys. The axons of the neurons in the area adjacent to the central canal, including the ventral DCN, where nociceptive neurons are located, have been shown to travel in the dorsal column to the gracile nucleus and in the ventrolateral quadrant to the reticular formation (Al-Chaer *et al.*, 1996; Wang *et al.*, 1999).

In our experiments, that the ANB were negative for nNOS was detected either by nNOS immunohistochemistry or by double-staining of the NADPH-d histochemistry combined with nNOS immunohistochemistry. Although the NADPH-d positive neurons were sometimes labeled by nNOS immunohistochemistry, there were several examples of non-colocalization. It has been argued that NADPH-d activity in the fixed brain is used as a marker for nNOS, and that NADPH-d and nNOS are actually the same enzyme (Dawson *et al.*, 1991). In contrast, Tracey *et al.* (1993) suggested that NOS represents only a fraction of the total cellular NADPH-d activity and that these activities are not always co-localized. Doone *et al.* (1999) also found some different aspects of NADPH-d staining and nNOS-immunoreactivity between the sympathetic preganglionic neurons in the thoracic and rostral lumbar segments and parasympathetic preganglionic neurons in the sacral segments of guinea pigs. The NADPH-d positive fibers of the LT only occurred in the S1-S3 segments, but for the most part, exhibited no nNOS-immunoreactivity. Similar results were obtained in the cat (Vizzard *et al.*, 1994). These results demonstrate that NADPH-d activity is not always a specific histochemical marker for the NO-containing neural structures. It is evident that nNOS has a NADPH-d activity (Tracey *et al.*, 1993), and that nNOS contains the amino acid sequences and co-factor binding sites needed to confer diaphorase activity (Bredt *et al.*, 1991). There are, however, enzymes with diaphorase activity that do not synthesize NO (Matsumoto *et al.*, 1993). Since the NBT reaction product is the result of the enzymatic reduction of NBT by NADPH-d, an increase in the amount of the reaction product indicates an increase in the enzymatic activity. Thus, NADPH-d histochemistry and the immunocytochemical labeling of nNOS do not absolutely label the same neuron population. The inferences relating NADPH-d histochemistry to the presence of NOS may be misleading since Young *et al.* (1997) suggest that NADPH-d activity neither indicates the existence of a specific NOS isoform nor clearly discriminates between NOS and other enzymes e.g., cytochrome P450 reductase, which may have some NADPH-d activity.

Both in horizontal and coronal sections the ANB displayed fibrous structures (approximately 200–300 μm) or a nerve fiber-like orientation (multifocal interruption of a long slender process by spheres). On the basis of these profiles, we suggest that they are a part of the neurite in the lumbosacral dorsal spinal cord. As for their origin, the question arises as to whether portions of the age-related structures come from the glia or blood vessels. The ANB were clearly distinguished from the glia and endothelium, as the size of typical ones was evidently bigger than the regular glia and they were not found in any detectable microblood vessels under the light microscope. It is, however, still possible that some of them reside in the glia and/or microvessels as fine remnants.

The features of the ANB are similar to those referred to as "neuroaxonal dystrophy (NAD) of primary sensory fibers" (Ma *et al.*, 1997, 2000). NAD occurs as a NADPH-positive spheroidal structure in the gracile nuclei of aged rats (Ma *et al.*, 1997) or in aged humans (Brannon *et al.*, 1967). From neuropathological studies, Ma *et al.* (2000) have shown that NADPH-d staining could be used to reveal the neuronal teriminal-pathy of aged conditions. In their experiments, NADPH-d positive large- and medium-sized cells were multipolar in shape with dendrites and axon terminals, together with a few dense fiber networks and evident in the gracile nucleus of aged rats (24 months old). The genesis as well as association to aging of the NADPH-positive NAD is, however, poorly understood. NAD is regarded as degenerated products of the primary sensory fiber originating from ascending terminals in the gracile (Ma *et al.*, 2000). Unilateral sciatic axotomy causes an increase in the nNOS expression as well as NADPH-d reactivity in the ipsilateral gracile nucleus of young rats, which increases in older rats with the normal aging process (Ma *et al.*, 2000). Typical spheroidal structures could then block axonal transport to give rise to morphological changes identical to denervation.

In our unpublished data, both the ANB and NAD were mostly spheroids, while some others had irregular shapes. The type 1 of the ANB were homogeously distributed throughout the dorsal column from all segments of the spinal cord to the gracile nuclei as shown by our series of spinal cord sections. The profiles and densities of NADPH-d staining in the type 1 are similar to those of NAD. The NADPH-d positive NAD in the gracile nuclei was, however, more densely stained than the ANB in the sacral DCN, because most of the NAD bodies stained earlier than the ANB (data not shown data). In addition, the type 2 of the ANB, with moderately-dense spheroidal or multiangular shapes and a central core and a peripheral halo, is distinct from the NADPH-positive

NAD. Therefore, the ANB may not be completely described as NAD. The ANB were distributed where the transganglionic fibers of the afferent pathway pass and terminate in the aging pathway of the autonomic and/or sensory system, which regulate the pelvic organ. No neuroanatomical linkage or connection between the ANB and NAD is known, but in either case some denervation-like changes due to interruption of the axonal transport are likely.

Mohammed and Santer (2001) reported that the total number of L6 and S1 dorsal root ganglia (DRG) cells as well as their diameters remain essentially constant from 3 to 24 months. These results have shown that the numbers of rat DRG cells do not change during adult life and that either the neurogenesis of DRG cells in adult rats or neuronal cell death in aged rats is unlikely to occur. Dering *et al.* (1996) suggested that, in the preganglionic neurons of the lumbar and sacral spinal cord of 4- and 24-month-old male rats, significant decreases occur in the number of dendritic branch points and the total dendritic length of the sympathetic preganglionic neurons in the aged rats, relative to the adult group. Recently, Chung *et al.* (2005) reported that a reduction in the number of nNOS-immunoreactive neurons occurs in the central autonomic nucleus and the superficial dorsal horn of the spinal cord in aged rats. In addition, the number and length of dendritic branches were significantly affected. Ranson *et al.* (2003) also reported that DCN and ILN of the lumbosacral spinal cords in aged rats exhibit notable depletions in neurotransmitter levels accompanied by axonal dystrophy. Further morphological studies into the origin and nature of the ANB should serve toward understanding the onset of age-related anomalous structures. We suggest that, with the progression of cellular loss in the lumbosacral dorsal spinal cord, portions of the neurites take the form of nNOS-negative and NADPH-d positive structures. In our experiment, the ANB indicated a novel structure, which uniquely occurs in aged rats, and which may account for the age-related dysfunction of the axonal transport in some pelvic organs.

In summary, the major new finding revealed by this study is that the NADPH-d positive bodies are present in the aged lumbosacral spinal cord, but not in young rats. From our morphological research, they might be a swelling of the transganglionic fibers of the LZ in the lateral dorsal marginal to the dorsal horn, superficial dorsal horn, ILN, and dorsal part of DCN in the lower lumbar and sacral spinal cord. On the basis of the main distribution obtained from NADPH-d staining, it appears that there is some relationship between the structures and age-related physical dysfunctions in the pelvic organs.

Acknowledgments

The authors acknowledge the expert advice of Assistant Professor Y. Aika regarding the stereological measurements, and the technical assistance of Miss Lingshu Kong using the system of the optical dissector.

References

Al-Chaer ED, Lawand NB, Westlund KN, Willis WD: Visceral nociceptive input into the ventral posterolateral nucleus of the thalamus: a new function for the dorsal column pathway. *J Neurophysiol* 76: 2661-2674 (1996).

Berkley KJ: A life of pelvic pain. *Physiol Behav* 86: 272-280 (2005).

Berkley KJ, Hubscher CH, Wall PD: Neuronal responses to stimulation of the cervix, uterus, colon, and skin in the rat spinal cord. *J Neurophysiol* 69: 545-556 (1993).

Brannon W, McCormick W, Lampert P: Axonal dystrophy in the gracile nucleus of man. *Acta Neuropathol (Berl)* 9: 1-6 (1967).

Bredt DS, Hwang PM,Glatt CE, Lowenstain C, Reed RR, Snyder SH: Cloned and expressed nitric oxide synthase structurally resembles cytochrome P-450 reductase. *Nature* 351: 714-718 (1991).

Chung YH, Kim D, Lee KJ, Kim SS, Kim KY, Cho DY, Sohn DS, Lee WB: Immunohistochemical study on the distribution of neuronal nitric oxide synthase-immunoreactive neurons in the spinal cord of aged rat. *J Mol Histol* 36: 325-329 (2005).

Cohen BA, Major MR, Huizenga BA: Pudendal nerve evoked potential monitoring in procedures involving low sacral fixation. *Spine* 16 (8 Suppl): S375-378 (1991).

Dawson TM, Bredt DS, Fotuhi M, Hwang PM, Snyder SH: Nitric oxide synthase and neuronal NADPH diaphorase are identical in brain and peripheral tissue. *Proc Natl Acad Sci* 88: 7797-7801 (1991).

Dering MA, Santer RM, Watson AH: Age-related changes in the morphology of preganglionic neurons projecting to the rat hypogastric ganglion. *J Neurocytol* 25: 555-563 (1996).

de Groat WC, Steers WD: Autonomic regulation of the urinary bladder and sexual organs. In: *Central regualtion of autonimic functions* (Loeway AD, Spyer KM, ed). Oxford University Press, New York, 1990 (p. 310-333).

Doone VG, Pelissier N, Manchester T, Vizzard AM: Distribution of NADPH-d and nNOS-IR in the thoracolumbar and sacrococcygeal spinal cord of the guinea pig. *J Auton Nerv Syst* 77: 98-113 (1999).

Honda CN: Visceral and somatic afferent convergence onto neurons near the central canal in the sacral spinal cord of the cat. *J Neurophysiol* 53: 1059-1078 (1985).

Liu Y, Tan H, Wan X, Zuo Z, Liu K: Spinal segment distribution of neural innervation related to houhai acupointand compared with zusanli and dazhui acupoints in domestic chicken. *Acta Acad Med Sin* 20: 154-160 (1998).

Lynn RB, Sankey SL, Chakder S, Rattan S: Colocalization of NADPII-diaphorase staining and VIP immunoreactivity in neurons in opossum internal anal sphincter. *Dig Dis Sci* 40: 781-791 (1995).

Ma S, Cornford ME, Vahabnezhad I, Wei S, Li X: Responses of nitric oxide sythase expression in the gracile nucleus to sciatic nerve injury in young and aged rats. *Brain Res* 855: 124-131 (2000).

Ma SX, Holley AT, Sandra A, Cassell MD, Abboud FM: Increased expression of nitric oxide synthase in the gracile nucleus of aged rats. *Neuroscience* 76: 659-663 (1997).

Matsumoto T, Masaki N, Pollock JS, Kuk JE, Forstermann U: A correlation between soluble brain nitric oxide synthase and NADPH-diaphorase activity is only seen after exposure of the tissue to fixative. *Neurosci Lett* 155: 61-64 (1993).

McKenna KE, Nadelhaft I: The organization of the pudental nerve in the male and female rat. *J Comp Neurol* 248: 532-549 (1986).

Mohammed HA, Santer RM: Total neuronal numbers of rat lumbosacral primary afferent neurons do not change with age. *Neurosci Lett* 304: 149-152 (2001).

Nadelhaft I, Vera PL: Neurons in the rat brain and spinal cord labeled after pseudorabies virus injected into the external urethral sphincter. *J Comp Neurol* 375: 502-517 (1996).

Persson K, Alm P, Johansson K, Larsson B, Andersson KE: Nitric oxide synthase in pig lower urinary tract: immunohistochemistry, NADPH diaphorase histochemistry and functional effects. *Br J Pharmacol* 110: 521-530 (1993).

Ranson RN, Dodds AL, Smith MJ, Santer RM, Watson AH: Age-associated changes in the monoaminergic innervation of rat lumbosacral spinal cord. *Brain Res* 972: 149-158 (2003).

Ricc AS: Topical spinal administration of a nitric oxidc synthase inhibitor prevents the hyper-reflexia associated with a rat model of persistent visceral pain. *Neurosci Lett* 187: 111-114 (1995).

Santer RM, Dering MA, Ranson RN, Waboso HN, Watson AH: Differential susceptibility to ageing of rat preganglionic neurons projecting to the major pelvic ganglion and of their afferent inputs. *Aut Neurosci Basic Clin* 96: 73-81 (2002).

Sie JA, Blok BF, De Weerd H, Holstege G: Ultrastructural evidence for direct projections from the pontine micturition center to glycine-immunoreactive neurons in the sacral dorsal gray commissure in the cat. *J Comp Neurol* 429: 631-637 (2001).

Spike RC, Todd AJ, Johnston HM: Coexistence of NADPH diaphorase with GABA, glycine, and acetylcholine in rat spinal cord. *J Comp Neurol* 335:320-333(1993).

Tamura M, Kagawa S, Kimura K, Kawanishi Y, Tsuruo Y, Ishimura K: Coexistence of nitric oxide synthase, tyrosine hydroxylase and vasoactive intestinal polypeptide in human penile tissue — a triple histochemical and immunohistochemical study. *J Urol* 153: 530-534 (1995).

Thor KB, Morgan C, Nadelhaft I, Houseton M, De Groat WC: Organization of afferent and efferent pathways in the pudendal nerve of the female cat. *J Comp Neurol* 288: 263-279 (1989).

Tracey WR, Nakane M, Pollock JS, Forstermann U: Nitric oxide synthases in neuronal cells, macrophages and endothelium are NADPH diaphorases, but represent only a fraction of total cellular NADPH diaphorase activity. *Biochem Biophys Res Commun* 195: 1035-1040 (1993).

Vizzard MA, Erdman SL, Erickson VL, Stewart RJ, Roppolo JR, De Groat WC: Localization of NADPH diaphorase in the lumbosacral spinal cord and dorsal root ganglia of the cat. *J Comp Neurol* 339: 62-75 (1994).

Vizzard MA, Erdman SL, Card JP, Roppolo JR, De Groat WC: Transnueronal labeling of neurons in the adult rat brain stem and spinal cord after injection of pseudorabies virus into the urethra. *J Comp Neurol* 355: 629-640 (1995).

Wang CC, Willis WD, Westlund KN: Ascending projections from the area around the spinal cord central canal: A Phaseolus vulgaris leucoagglutinin study in rats. *J Comp Neurol* 415: 341-367 (1999).

Wang HF, Shortland P, Park MJ, Grant G: Retrograde and transganglionic transport of horseradise peroxidase-conjugated cholera toxin B subunit, wheatgerm agglutinin and isolectin B4 from *Griffonia simplicifolia I* in primary afferent neurons innervating the rat urinary bladder. *Neuroscience* 87: 275-288 (1998).

West MJ, Gundersen HJG: Unbiased stereological estimation of the number of neurons in the human hippocampus. *J Comp Neurol* 296: 1-22 (1990).

Willis WD, Al-Chaer ED, Quast MJ, Westlund KN: A visceral pain pathway in the dorsal column of the spinal cord. *Proc Natl Acad Sci* 96: 7675-7679 (1999).

Young HM, O'Brien AJ, Furness JB, Ciampoli D, Hardwick JP, McCabe TJ, Narayanasami R, Masters BS, Tracey WR: Relationships between NADPH diaphorase staining and neuronal, endothelial, and inducible nitric oxide synthase and cytochrome P450 reductase immunoreactivities in guinea-pig tissues. *Histochem Cell Biol* 107: 19-29 (1997).

Zhang RD, Wen XH, Kong LS, Deng XZ, Peng B, Huang AP, Wan Y and Yang ZW: A quantitative (stereological) study of the effects of experimental unilateral cryptorchidism and subsequent orchiopexy on spermatogenesis in adult rabbit testis. *Reproduction* 124: 95-105 (2002).